JVI Journals.ASM.org

Generation of Live Attenuated Influenza Virus by Using Codon Usage Bias

Rebecca L. Y. Fan,[a] Sophie A. Valkenburg,[a] Chloe K. S. Wong,[a] Olive T. W. Li,[a] John M. Nicholls,[b] Raul Rabadan,[c] J. S. Malik Peiris,[a] Leo L. M. Poon[a]

Centre of Influenza Research and School of Public Health, The University of Hong Kong, Hong Kong, SAR, China[a]; Department of Pathology, The University of Hong Kong, Hong Kong, SAR, China[b]; Department of Systems Biology and Department of Biomedical Informatics, Columbia University College of Physicians and Surgeons, New York, New York, USA[c]

ABSTRACT

Seasonal influenza epidemics and occasional pandemics threaten public health worldwide. New alternative strategies for generating recombinant viruses with vaccine potential are needed. Interestingly, influenza viruses circulating in different hosts have been found to have distinct codon usage patterns, which may reflect host adaptation. We therefore hypothesized that it is possible to make a human seasonal influenza virus that is specifically attenuated in human cells but not in eggs by converting its codon usage so that it is similar to that observed from avian influenza viruses. This approach might help to generate human live attenuated viruses without affecting their yield in eggs. To test this hypothesis, over 300 silent mutations were introduced into the genome of a seasonal H1N1 influenza virus. The resultant mutant was significantly attenuated in mammalian cells and mice, yet it grew well in embryonated eggs. A single dose of intranasal vaccination induced potent innate, humoral, and cellular immune responses, and the mutant could protect mice against homologous and heterologous viral challenges. The attenuated mutant could also be used as a vaccine master donor strain by introducing hemagglutinin and neuraminidase genes derived from other strains. Thus, our approach is a successful strategy to generate attenuated viruses for future application as vaccines.

IMPORTANCE

Vaccination has been one of the best protective measures in combating influenza virus infection. Current licensed influenza vaccines and their production have various limitations. Our virus attenuation strategy makes use of the codon usage biases of human and avian influenza viruses to generate a human-derived influenza virus that is attenuated in mammalian hosts. This method, however, does not affect virus replication in eggs. This makes the resultant mutants highly compatible with existing egg-based vaccine production pipelines. The viral proteins generated from the codon bias mutants are identical to the wild-type viral proteins. In addition, our massive genome-wide mutational approach further minimizes the concern over reverse mutations. The potential use of this kind of codon bias mutant as a master donor strain to generate other live attenuated viruses is also demonstrated. These findings put forward a promising live attenuated influenza vaccine generation strategy to control influenza.

Seasonal influenza strikes every year, and the threat of avian influenza outbreaks and worldwide pandemics together make influenza a significant health risk to the general public, particularly young children, pregnant women, the elderly, and patients with underlying medical conditions (1). Vaccination remains one of the best control measures against influenza. However, currently licensed inactivated and live attenuated influenza vaccines have their limitations. Therefore, new options for vaccine development are needed.

Vaccination with an updated virus strain is required every year in response to the frequent occurrence of antigenic drift. Even when the vaccine strain antigenically matches the circulating strain, the trivalent inactivated vaccine can provide partial protection only in some healthy adults (2). The 2014-2015 winter seasonal influenza epidemic in many areas of the Northern Hemisphere showed us that the mismatch between the vaccine H3N2 strain and the dominant antigenically drifted H3N2 virus resulted in a very low vaccine effectiveness (3), resulting in excess mortality in people over 65 years old. Young children and the elderly, who are more likely to develop severe complications, are often less protected by inactivated vaccines (2, 4, 5). A recombinant protein-based influenza vaccine was recently approved for use in people ranging from 18 to 49 years of age; however, it is less immunogenic in children (6–8). Nonetheless, recombinant protein vaccines are useful for individuals with egg allergy. Live attenuated influenza vaccines (LAIVs) have been found to be superior to the standard inactivated vaccine by a few measures, such as administration by noninvasive means and stimulation of secretory mucosal IgA and cytotoxic T cell responses (5, 9), especially in children (10, 11). However, safety concerns over LAIVs have been raised, as the cold-adapted phenotype is controlled by only 5 nonsilent mutations (12). Therefore, the public still awaits a more universal in-

Received 3 June 2015 **Accepted** 5 August 2015

Accepted manuscript posted online 12 August 2015

Citation Fan RLY, Valkenburg SA, Wong CKS, Li OTW, Nicholls JM, Rabadan R, Peiris JSM, Poon LLM. 2015. Generation of live attenuated influenza virus by using codon usage bias. J Virol 89:10762–10773. doi:10.1128/JVI.01443-15.

Editor: S. Perlman

Address correspondence to Leo L. M. Poon, llmpoon@hku.hk.

Supplemental material for this article may be found at http://dx.doi.org/10.1128/JVI.01443-15.

fluenza vaccine that is safe and able to elicit potent long-term humoral and cellular immune responses. Ideally, a universal vaccine should also be capable of inducing some cross-subtype protection.

Codon usage bias refers to the unequal frequency in the usage of synonymous codons (13), which can be found in many species, including influenza viruses (14–17). In our previous studies, the codon usage patterns were found to be different between human and avian influenza viruses (16). Two models have been proposed to explain the codon usage bias observed. The mutational (or neutral) model is based on the nonrandomness of mutations in certain regions, such as GC-rich regions in RNA viruses. Recent studies suggest that this might help the virus escape host antiviral responses (13, 16, 18, 19). In the translation (or selection) model, codon usage is adapted to the host tRNA abundance in order to enhance translation and fitness (16, 18–20).

The different codon usage biases observed in human and avian influenza viruses have prompted us to hypothesize that host adaptation might shape the codon usage of influenza viruses. Indeed, there is evidence that the incorporation of synonymous mutations into influenza virus might lead to virus attenuation (18, 21–23). Previous studies on influenza virus have made use of deoptimized codon pair mutations or misrepresented mammalian codons to generate attenuated viruses carrying 1 to 3 mutated viral segments (24–26). In this study, we generated a live attenuated human seasonal influenza virus containing an avian influenza virus codon usage bias. Multiple silent mutations were introduced into all 8 segments by *de novo* synthesis. Vaccination with a single dose of this codon mutant virus conferred protection against homologous and heterologous viral challenge, and this mutant could be used as a vaccine master donor strain.

MATERIALS AND METHODS

Design of a human influenza virus with avian influenza virus-like codon bias sequences. Influenza A/Brisbane/59/2007 (H1N1) (BR59), representing a human influenza virus strain previously used for vaccine production, was used as the prototype virus in this study. Only the largest open reading frame (ORF) of each segment was selected for the analysis. A data set for each segment from viruses that are of human or avian origin was established in our previous studies (16). The codon usage bias observed from each segment-specific data set was compared to that observed from the corresponding counterpart (e.g., human influenza virus PB2 versus avian influenza virus PB2). We compared the segment-specific codon usage frequency of wild-type (WT) BR59 with the average codon usage frequency deduced from the corresponding avian influenza virus sequences. This analysis allowed us to determine the number of mutations required to be introduced into the prototype virus to change its codon bias from human influenza virus-like to avian influenza virus-like (Table 1; see also Supplemental Data S1 in the supplemental material). In order to avoid affecting critical viral RNA signals essential for virus replication, mutations were introduced into the regions that are known to not be involved in viral RNP (vRNP) packaging and splicing (27–29). Sequence regions with out-of-frame ORFs (e.g., PB1 and PB1-F2 ORFs) were also excluded from mutagenesis. With the exception of the critical regions indicated above (see Supplemental Data S2 in the supplemental material), the mutations were randomly yet evenly distributed in the targeted open reading frame (see Supplemental Data S1 in the supplemental material). Specifically, these mutations were introduced into sites that are highly conserved at the amino acid sequence level (>99%) but not at the nucleotide sequence level. This was to minimize the risk of (i) introducing mutations into potential mutational hot spots (i.e., highly polymorphic amino acid positions) or (ii) disrupting potential critical RNA signals (i.e., highly conserved codon positions). After introducing the designed 373 nucleotide mutations into 351 codons in the viral genome (see Supplemental Data S3 in the supplemental material), the genome of the resultant BR59 mutant encoded wild-type BR59 viral proteins but the largest ORF of each segment had an avian influenza virus-like viral codon usage bias. The nucleotide and dinucleotide usage frequencies of the mutated ORFs were generally found to be more similar to those observed from the avian influenza virus sequence data set (see Supplemental Data S4 and S5 in the supplemental material). In addition, the minimum free energy of the mutated genes was also found to be similar to that of avian influenza virus sequences reported previously (30) (see Supplemental Data S6 in the supplemental material). In contrast, many of the parameters deduced from wild-type BR59 were generally found to be distinct from those of avian influenza viruses (see Supplemental Data S4 to S6 in the supplemental material). Both the WT and mutated viral RNA segments were then synthesized commercially (GenScript).

TABLE 1 Construction of influenza virus with avian influenza virus codon usage bias

Segment	No. (%) of mutations	
	Nucleotides[a]	Codon[b]
PB2	62 (2.65)	62 (8.17)
PB1	77 (3.29)	69 (9.11)
PA	65 (2.91)	61 (8.52)
HA	46 (2.59)	38 (6.73)
NP	31 (1.98)	30 (6.02)
NA	47 (3.21)	47 (10.00)
M	27 (2.63)	27 (10.71)
NS	18 (2.02)	17 (7.39)
Total	373 (2.74)	351 (8.26)

[a] Percentages were calculated by dividing the number of nucleotide mutations by the number of nucleotides for the full length of the respective segment.
[b] Percentages were calculated by dividing the number of codon mutations by the number of amino acids of the corresponding protein. For the PB1, M, and NS segments, data for the minor protein products PB1-F2, PB1-N40, PA-X, M2, and NS2 were excluded from the calculations, as no mutations were introduced into those regions.

Corresponding analysis of influenza virus sequences. Corresponding analysis is a type of multivariate analysis that allows a geometrical representation of a data set with multiple parameters. We performed corresponding analysis of the relative synonymous codon usage (RSCU) of avian and human influenza virus sequences in this study as previously described by us (16). The first three eigenvectors from each analysis were used to incorporate most information from the data sets and were used as axes for graphical presentation. Graphs were plotted using SigmaPlot (version 10.0) software (Systat Software Inc.).

Cells and viruses. MDCK, 293T, and A549 cells were maintained in minimum essential medium (MEM), while DF1 cells were maintained in Dulbecco's modified Eagle medium (DMEM). Both MEM and DMEM were supplemented with 1% penicillin and streptomycin (P/S) and 10% fetal bovine serum (FBS). All cells were kept in a humidified incubator with 5% CO_2 at 37°C. As listed in Table 2, WT BR59 virus, a mutant virus containing 8 mutated segments (8-mut), and mutant viruses containing 1 to 4 mutated segments were generated by reverse genetics techniques (31). Recombinant viruses consisting of 6 internal BR59 wild-type or mutant genes and hemagglutinin (HA) and neuraminidase (NA) from A/Puerto Rico/8/34 (H1N1) (PR8) or A/HK/1/68 (H3N2) (HK68) were also rescued (Table 3). To generate a more pathogenic virus for viral challenge experiments, mouse-adapted WT (MA-WT) BR59 virus was rescued by introducing 3 site-directed mutations (T89I, N125T, and D221G in the HA gene) that are known to increase virus pathogenicity in mice (32). PR8 was also rescued by reverse genetics (31). A mouse-adapted A/HK/1/68 clone, MA20C (HK68-MA20C; H3N2), was used for heterosubtypic virus

TABLE 2 Codon bias mutants generated in this study

Virus	Segment[a]							
	PB2	PB1	PA	HA	NP	NA	M	NS
WT	WT	WT	WT	WT	WT	WT	WT	WT
8-mut	M	M	M	M	M	M	M	M
PB2 mutant	M	WT	WT	WT	WT	WT	WT	WT
PB1 mutant	WT	M	WT	WT	WT	WT	WT	WT
PA mutant	WT	WT	M	WT	WT	WT	WT	WT
HA mutant	WT	WT	WT	M	WT	WT	WT	WT
NP mutant	WT	WT	WT	WT	M	WT	WT	WT
NA mutant	WT	WT	WT	WT	WT	M	WT	WT
M mutant	WT	WT	WT	WT	WT	WT	M	WT
NS mutant	WT	WT	WT	WT	WT	WT	WT	M
PB2, PB1, PA, NP mutant	M	M	M	WT	M	WT	WT	WT
HA, NA, M mutant	WT	WT	WT	M	WT	M	M	WT
HA, NA mutant	WT	WT	WT	M	WT	M	WT	WT
M, NS mutant	WT	WT	WT	WT	WT	WT	M	M

[a] WT, wild-type segment; M, mutated segment.

TABLE 3 Recombinant viruses obtained using BR59 as the master donor strain

Virus	Origin of PB2, PB1, PA, NP, M, and NS	Origin of HA and NA
WT+PR8-HN	BR59 WT	PR8
mut+PR8-HN	BR59 mutant	PR8
WT+HK68-HN	BR59 WT	HK68
mut+HK68-HN	BR59 mutant	HK68

challenge, and it was a generous gift from E. Brown (University of Ottawa, Ottawa, Ontario, Canada) (33). All viruses were amplified in embryonated eggs or MDCK cells, and their identities were confirmed by sequencing. Viral titers were determined by standard plaque assay on MDCK cells.

Growth kinetics experiments. Confluent cells were infected at a multiplicity of infection (MOI) of 0.001 for MDCK cells and an MOI of 0.01 for A549 cells in duplicate. Cells were incubated in infection medium supplemented with 1% P/S and tosyl phenylalanyl chloromethyl ketone (TPCK)-trypsin (1 μg/ml for MDCK cells, 0.5 μg/ml for A549 cells). The supernatant was harvested at 24, 48, or 72 h postinfection. For experiments using embryonated eggs, 100 PFU of viruses was inoculated into allantoic fluid. At 24, 48, or 72 h postinfection, the allantoic fluid was collected. Experiments were carried out at 37°C unless stated otherwise. Viral titers were determined by plaque assays on MDCK cells.

Mouse experiments. Specific-pathogen-free 4- to 9-week-old female BALB/c mice were infected intranasally with 25 μl of viruses. Body weights were monitored daily, and mice with a body weight loss of more than 25% were euthanized. To assess viral replication in lungs, lung tissues were harvested at days 3 and 7 postinfection and homogenized for titration by the 50% tissue culture infective dose ($TCID_{50}$) assay using MDCK cells. The values of the numbers of $TCID_{50}$s per gram were determined using the Reed and Muench method. All experiments with mice were carried out at the Laboratory Animal Unit of The University of Hong Kong and approved by the Committee on the Use of Live Animals in Teaching and Research, The University of Hong Kong.

Immune response assays. To determine the level of virus-neutralizing serum antibodies in mice, serum was harvested in MiniCollect tubes (Greiner Bio-One) at day 28 postinfection, followed by centrifugation and heat inactivation (56°C for 30 min). A microneutralization assay was performed using MDCK cells with 100 $TCID_{50}$s of viruses (34). The reciprocal of the highest dilution of serum that neutralized at least 50% of virus infectivity was taken as the titer. Immune cell profiling of cells isolated from bronchoalveolar lavage (BAL) fluid harvested at day 7 postinfection was performed as described previously (35). Briefly, after Fc receptor blocking, cells were stained with 2 mixtures of monoclonal antibodies (all BioLegend) for innate and adaptive immune cells. Mixture 1 consisted of F4/80-phycoerythrin (PE), I-AE–peridinin chlorophyll protein (PerCP)–Cy5.5, CD11b-allophycocyanin (APC)-Cy7, Gr1-PE-Cy7, IA8-APC, CD11c-fluorescein isothiocyanate (FITC), and DAPI (4′,6-diamidino-2-phenylindole). Mixture 2 consisted of CD3-APC, CD4-APC-Cy7, CD8-PerCP-Cy5.5, Dx5-FITC, γδT-PE, B220-PE-Cy7, and DAPI. Flow cytometry analysis was performed for cell type identification.

The interferon responses of infected A549 cells were measured by determination of the level of expression of beta interferon mRNAs using quantitative PCR (qPCR). A549 cells were infected with viruses at an MOI of 5 in triplicate. At 4 and 8 h postinfection, total cellular RNA was extracted using an RNeasy minikit (Qiagen) and DNase treatment using Turbo DNA-free DNase treatment and removal reagents (Ambion). mRNA molecules were reverse transcribed with an oligo(dT) primer and SuperScript II reverse transcriptase (Life Technologies). Gene-specific primers were used for amplification and quantification of cDNAs of beta interferon (36) and β-actin (37) in a real-time PCR system (7500; Applied Biosystems) (for beta interferon, 20 s at 95°C, followed by 40 cycles of 3 s at 95°C and 30 s at 60°C; for β-actin, 20 s at 95°C, followed by 40 cycles of 3 s at 95°C and 30 s at 64°C). A melting curve analysis (60°C to 95°C, 0.1°C/s) of the amplified products was also performed to determine the specificity of the assay. Diluted plasmids carrying the target sequences were used to generate standard curves. The levels of beta interferon mRNA expression were normalized by the level of β-actin expression.

Vaccine efficacy study. Groups of 12 female BALB/c mice were infected intranasally with 25 μl of viruses or mock vaccinated with phosphate-buffered saline (PBS). Treated mice were challenged with MA-WT virus, PR8, HK68-MA20C (33), or PBS (mock infection) at 28 days postvaccination. Body weight loss was monitored daily for 14 days ($n = 6$). At days 3 and 7 postchallenge, lungs ($n = 3$) were harvested from each group for viral titration and immunohistochemistry analysis. For viral titration, lung tissues were homogenized and titrated by the $TCID_{50}$ assay using MDCK cells. For immunohistochemistry analysis, tissues were fixed in 10% formalin and processed as described previously (38). Tissues were stained with monoclonal antibody against the NP (clone HB65; ATCC) of influenza A virus.

Protein expression and Western blotting. A549 and DF1 cells infected at an MOI of 5 and whole-cell lysates were harvested at various postinfection points as indicated below. Proteins were resolved in 12% SDS-polyacrylamide gels. Western blot analysis was performed using primary antibodies to one of the following: PB2 (catalog number vN19; Santa Cruz), PB1 (catalog number F5-19; BEI Resources), PA (a generous gift from Ervin Fodor, University of Oxford), HA (catalog number ab91531; Abcam), NP (catalog number C43; Abcam), NA (catalog number ab21304; Abcam), M1 (catalog number GA2B; Santa Cruz), NS1 (catalog number 23-1; Santa Cruz), and β-actin (catalog number C4; Santa Cruz). β-Actin levels were used as loading controls. Primary antibodies were detected using corresponding IRDye-conjugated secondary antibodies (LI-COR), and signals were quantified by use of an Odyssey CLx infrared imaging system.

Data and statistical analyses. Data were analyzed by Prism (version 6) software (GraphPad). The Student *t* test was carried out, and *P* values of less than 0.05 were considered significant.

RESULTS

Construction of influenza virus with avian influenza virus codon bias. Seasonal human influenza virus BR59 (H1N1) was used as the prototype virus for this study. This human H1N1 virus lineage has circulated in humans for decades and was confirmed to have a codon bias which is distinct from that of avian influenza virus strains (16). To convert the largest ORF of each viral segment of BR59 from having a codon bias of human viruses to one similar

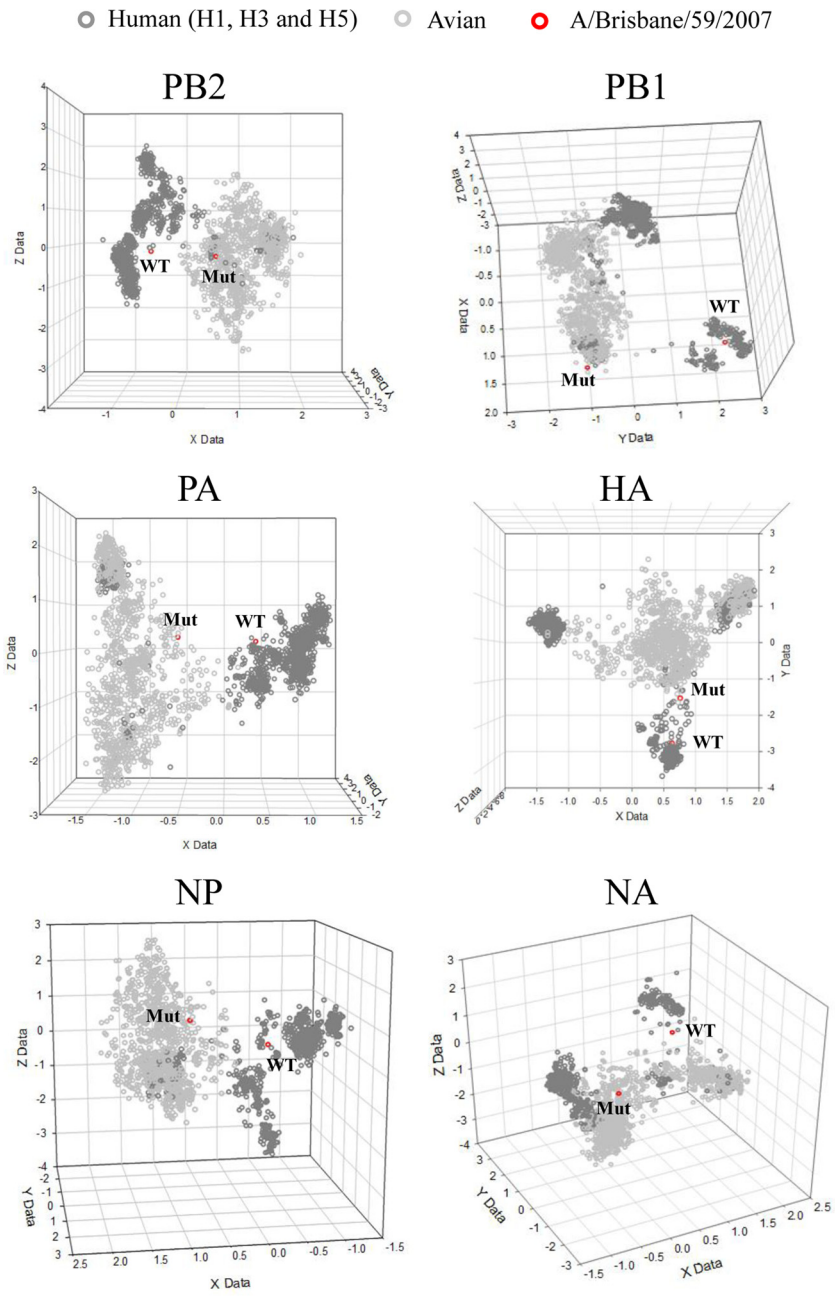

FIG 1 Corresponding analyses of human (seasonal H1, H3, and H5) and avian influenza viruses. Each dot presents a viral sequence. The arbitrary distance between 2 dots in the 3-dimensional space represents the difference of the RSCU values between 2 particular viral sequences in corresponding analysis. The locations of WT and mutated (Mut) A/Brisbane/59/2007 viral sequences are indicated. The M1 and NS1 viral sequences were excluded for graphical representation due to their short ORFs (16). The scales on the *x*, *y*, and *z* axes are in arbitrary units generated by corresponding analyses, and the weight of each codon in the different segments varies in these axes (16).

to that of avian viruses, we compared each of its viral segments to those of avian influenza viruses (see Materials and Methods). A total of 373 nucleotide mutations corresponding to 351 codon mutations were introduced into the BR59 genome (Table 1; see Supplemental Data S1 and S3 in the supplemental material), and all of these nucleotide changes were silent mutations. The mutated sequences were confirmed to have codon usage biases similar to those of avian influenza virus sequences by corresponding analysis (Fig. 1). We also studied the nucleotide frequency, dinucleotide frequency, and free energy of the mutated ORFs (see Materials and Methods). In general, the mutated sequences were found to be more similar to those observed from avian influenza virus sequences in many of these parameters (see Supplemental Data S4 to S6 in the supplemental material).

Synthetic DNAs for the WT and mutated viral genomes were chemically synthesized, and recombinant viruses were generated by reverse genetics (31). Wild-type BR59 virus, a mutant with 8 mutated segments (referred to here as 8-mut), and mutants with 1

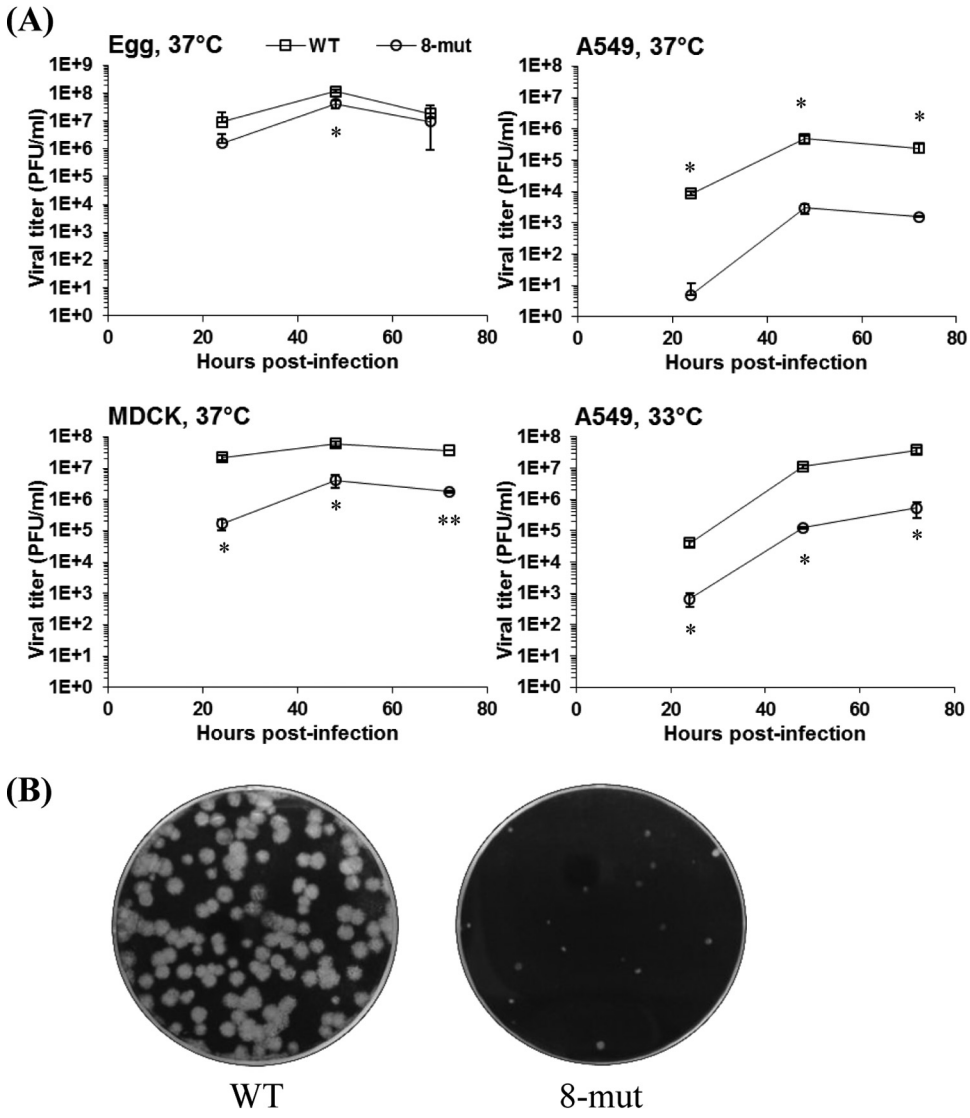

FIG 2 Growth properties of the codon bias mutant in mammalian and avian systems. (A) The growth kinetics of WT and 8-mut viruses were characterized in embryonated eggs (100 PFU) and MDCK cells (MOI = 0.001) at 37°C and A549 cells (MOI = 0.01) at 37°C and 33°C. *, $P < 0.05$; **, $P < 0.001$. (B) Plaque sizes of WT and 8-mut viruses in MDCK cells. Cells were infected with WT and 8-mut viruses, and cells were fixed and stained with crystal violet at 3 days postinfection.

to 4 mutated segments were generated in this study (Table 2). The rescued viruses were amplified in embryonated eggs, and the identities of these viruses were confirmed by sequencing. In addition, the WT and 8-mut viruses were subjected to full-genome sequencing, and no undesirable mutation was detected in these two viruses.

Characterization of the 8-mut virus in *in vitro* and *in vivo* models. The replication kinetics of the WT and 8-mut viruses were determined in mammalian cells (MDCK and A549 cells) and embryonated eggs at 37°C. The replication of 8-mut virus was found to be attenuated (the titer was >1 log unit less) in MDCK cells (Fig. 2A, bottom left). In addition, the plaque size of the 8-mut virus was found to be smaller than that of the WT in MDCK cells (Fig. 2B). The 8-mut virus was even more attenuated in A549 cells (Fig. 2A, top right), and 8-mut virus titers were at least 2 log units less than those of the WT. Moreover, similar attenuation was also observed in A549 cells at 33°C (Fig. 2A, bottom right), indicating that the 8-mut virus is not a temperature-sensitive mutant. Interestingly, the 8-mut virus was found to have replication kinetics comparable to those of the wild type in eggs (Fig. 2A, top left, <0.5-log-unit difference in titer at any time point).

Since the 8-mut virus was highly attenuated in mammalian cells, we evaluated whether the same attenuation could also be found in mice. Groups of 5 mice were infected intranasally with the highest achievable titer (6.75×10^5 PFU/dose) of the WT or 8-mut virus. Mice infected with the WT virus showed transient weight loss, while those infected with the 8-mut virus did not show any weight loss or sickness (Fig. 3A). In fact, the infections caused by the 8-mut virus were very mild, and the weights of these mice were found to be similar to those normally observed for uninfected mice (data not shown). To examine virus replication in mice, the viral titers in lung tissues harvested at days 3 and 7 postinfection were determined by titration. The viral titers observed for mice infected with the 8-mut were 40-fold lower than

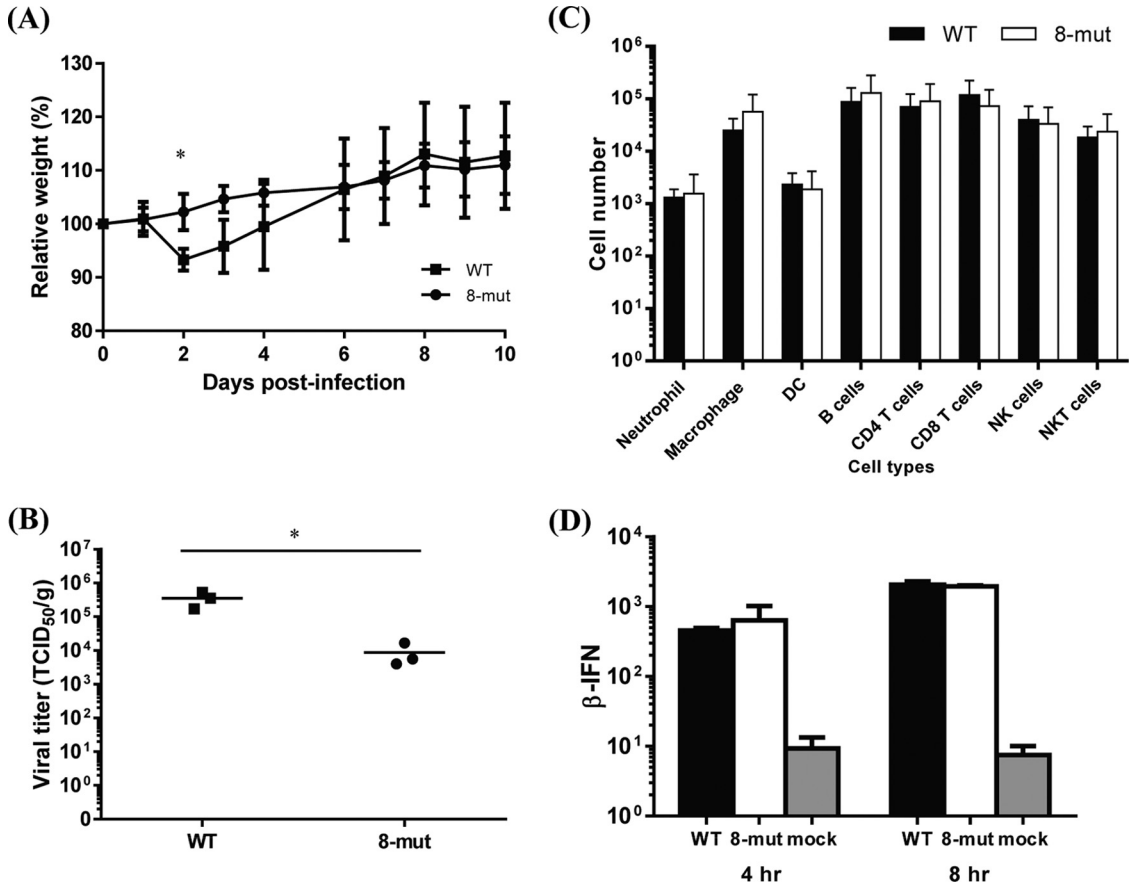

FIG 3 Characterization of viruses in mice and immune response. Groups of BALB/c mice were infected intranasally with 6.75×10^5 PFU of WT or 8-mut virus. (A) The body weights of 5 mice were monitored for 10 days, and data represent means ± SDs. *, $P < 0.05$. (B) Lungs from 3 mice were harvested at 3 days postinfection, and viral titers were determined by a standard $TCID_{50}$ assay on MDCK cells. Symbols represent data from individual mice. *, $P < 0.05$. (C) BAL fluid was harvested at day 7 postinfection, stained with a mixture of monoclonal antibodies for innate and adaptive immune cells, and analyzed by flow cytometry. Data represent total cell numbers (means ± SDs). DC, dendritic cells. (D) A549 cells were infected with the WT or 8-mut virus at an MOI of 5 for 4 and 8 h. Beta interferon (β-IFN) mRNA expression was measured by qPCR, and the level of expression was normalized to the level of β-actin expression and expressed as the mean ± SD.

those observed for the WT-infected mice (Fig. 3B), indicating that the 8-mut virus is also attenuated in mice. No infectious virus was detected in mice infected with the WT or 8-mut virus at day 7 postinfection.

To determine whether the 8-mut virus, which had an attenuated phenotype in mice, was capable of inducing neutralizing antibodies *in vivo*, serum samples collected from mice at 28 days postinfection were examined by a microneutralization assay. Mice infected with the WT or 8-mut virus were found to have similar neutralizing antibody titers against both the WT and 8-mut viruses (antibody titers, 1:640 to 1:1,280). In addition, BAL fluid was collected from infected mice at day 7 postinfection for immune cell profiling (Fig. 3C), and both WT and 8-mut virus infections were found to produce indistinguishable immune cell profiles in mice.

The interferon response in infected A549 cells was measured by quantifying cellular beta interferon mRNA using quantitative reverse transcription-PCR. At both 4 and 8 h postinfection, WT and 8-mut virus infections induced comparable levels of expression of beta interferon mRNA (Fig. 3D). These results altogether suggest that the 8-mut virus was attenuated in mammalian systems but could still induce potent immune responses.

Priming with the 8-mut virus vaccine protects mice from viral challenge. In order to determine whether the 8-mut virus can induce sufficient immune protection in mice, infected mice were subsequently subjected to a homologous viral challenge. As the original WT (BR59) virus caused only mild weight loss in mice (Fig. 3A), a more pathogenic mouse-adapted BR59 virus (MA-WT) carrying 3 HA mutations (T89I, N125T, and D221G) was generated (32). The MA-WT virus was serologically identical to the WT virus in microneutralization assays (data not shown), and mice infected with the MA-WT virus had more severe symptoms and weight loss than those infected with the WT virus. Therefore, the MA-WT virus was used in the virus challenge study.

Four-week-old BALB/c mice ($n = 6$) were vaccinated intranasally with 6.75×10^5 PFU of the 8-mut virus. Vaccinated mice or mock-vaccinated mice (primed with PBS only) were challenged with 4.3×10^5 PFU of MA-WT virus at day 28 postvaccination. The mock-vaccinated mice displayed symptoms of infection and had significant weight loss (Fig. 4A). In contrast, the vaccinated mice showed no symptoms and no weight loss. Lung tissues from treated mice were harvested at days 3 and 7 postchallenge for viral titration and immunohistochemistry staining. High levels of virus replication were detected in mock-treated mice but not in vacci-

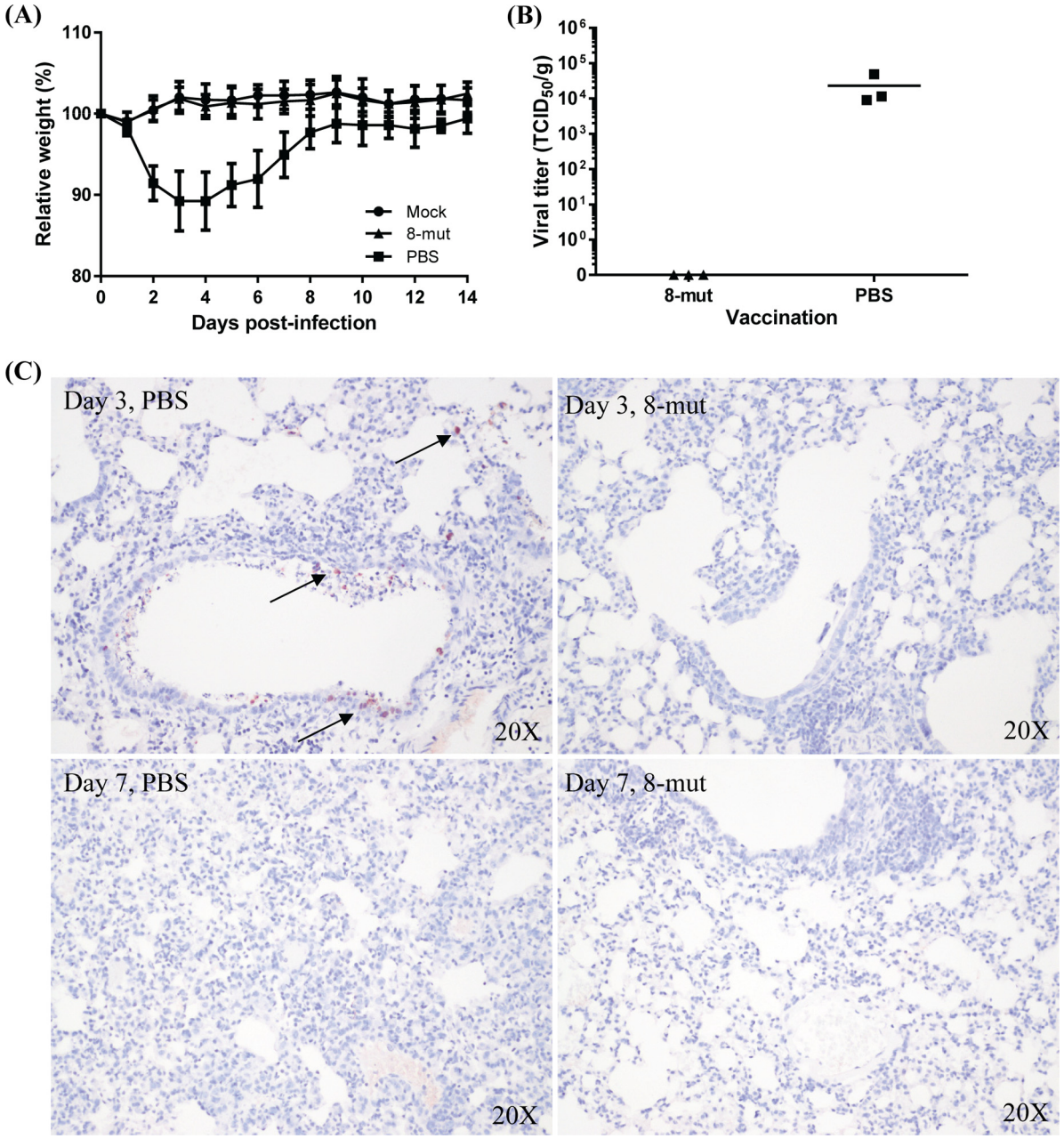

FIG 4 Protective effects caused by the 8-mut virus. BALB/c mice were vaccinated intranasally with PBS or 6.75×10^5 PFU of the 8-mut virus. At day 28 postvaccination, mice were challenged with 4.3×10^5 PFU of MA-WT virus or underwent mock challenge as a control. (A) The loss of body weight of 6 mice was monitored for 14 days, and data represent means ± SDs. (B) Lungs were harvested from 3 mice at 3 days postchallenge, and viral titers were determined by a standard $TCID_{50}$ assay on MDCK cells. Symbols represent data from individual mice. (C) Immunohistochemistry staining of selected lung tissues. Mice were vaccinated with PBS (left) or the 8-mut virus (right). Lung tissues were harvested at day 3 (top) or day 7 (bottom) postchallenge. Arrows, representative influenza A virus NP-positive cells.

nated mice at day 3 postinfection (Fig. 4B). In addition, cells expressing influenza virus NP proteins were detected only in mock-treated mice (Fig. 4C) at day 3 postchallenge. NP-positive cells were not detected in either group at day 7 postchallenge. However, consolidation of the lung was observed only in mock-vaccinated mice and not in mice vaccinated with the 8-mut virus (Fig. 4C).

We further evaluated whether vaccination with the 8-mut virus can confer protection against heterologous viral challenge. At day 28 postvaccination, mice were challenged with a heterologous H1N1 virus (PR8) or a heterosubtypic mouse-adapted H3N2 virus (HK68-MA20C). In the PR8 challenge experiment, all mock-treated mice had a body weight loss of more than 25% and were sacrificed (PR8 was 100% lethal) (Fig. 5A and B). In contrast, except for 1 mouse, the other 5 mice in the vaccinated group survived and showed a body weight loss of less than 16% (Fig. 5A and B). In the HK68-MA20C challenge experiment, all mice in both groups survived, but the mice in the vaccinated group had much less body weight loss and earlier recovery than mice in the

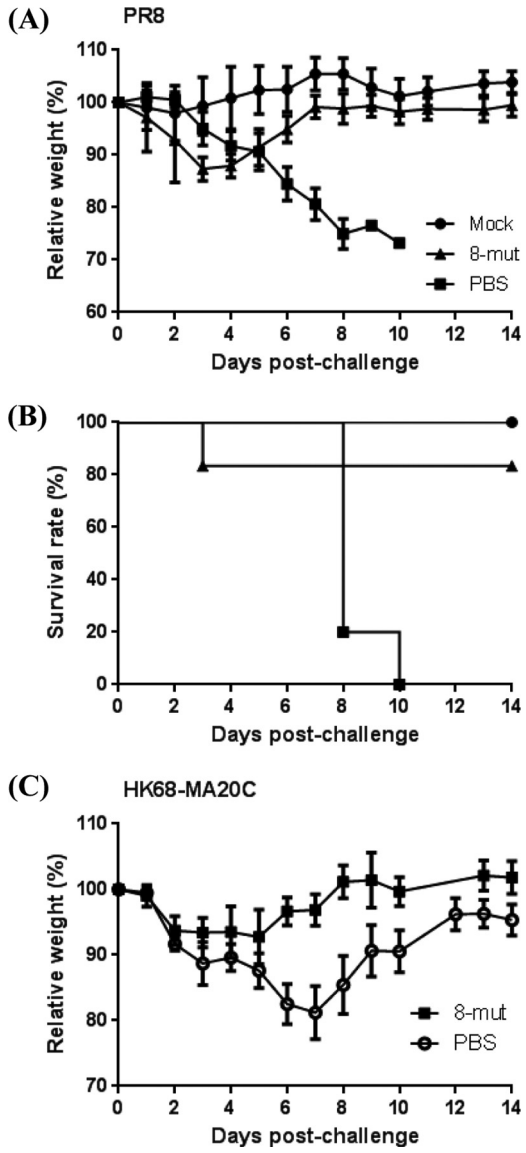

FIG 5 Heterologous protective effects caused by the 8-mut virus. BALB/c mice were vaccinated intranasally with PBS (mock-vaccinated control) or 6.75×10^5 PFU of 8-mut virus. At day 28 postvaccination, mice were challenged with PR8 (100 50% lethal doses, 2.1×10^4 PFU) (A, B) or HK68-MA20C (6.71×10^5 PFU) (C) or underwent mock challenge as a control (A to C). (A, C) The loss of body weight of 6 mice was monitored for 14 days, and data represent means ± SDs. (B) Survival rate after challenge with PR8.

mock-treated group (Fig. 5C). Overall, these results suggest that the 8-mut virus can induce immunological protection against homologous and heterologous influenza virus challenge.

Mutant virus as a vaccine master donor strain candidate. To investigate if the mutant virus could be used as a vaccine master donor strain, recombinant viruses whose genomes contained wild-type or mutated segments of the 6 internal genes of BR59 and the HA and NA segments from PR8 or HK68 were rescued (Table 3). Virus replication kinetics were studied in A549 cells and eggs at 37°C. For viruses with PR8 HA and NA, the codon bias mutant virus was significantly attenuated in A549 cells, but its replication rate was comparable to that of the virus with the BR59 background in eggs (Fig. 6A). This codon bias mutant (mut+PR8-HN) was also confirmed to be attenuated *in vivo*. All mice infected by this mutant survived the infection (see Supplemental Data S7 in the supplemental material). In contrast, all mice infected with the control virus (WT+PR8-HN) died from the infection. For viruses with HK68 HA and NA, the maximum titer of the progeny of the codon bias mutant virus was moderately less than that achieved with the virus with the BR59 background (<0.5 log unit at 48 h postinfection), but the codon bias mutant was even more attenuated in A549 cells, as expected (Fig. 6B).

The promising results presented above prompted us to further evaluate the vaccine potential of the mutant virus in mice. Since BR59 (H1N1) and HK68 (H3N2) are different viral subtypes, we focused on the mut+HK68-HN virus, which could better demonstrate the protection induced by the surface HA and NA proteins. Groups of 6 mice were vaccinated intranasally with 1×10^5 PFU of the mut+HK68-HN virus and challenged with 6.71×10^5 PFU of HK68-MA20C at 28 days postvaccination. Vaccinated mice had no sign of morbidity (i.e., symptoms and weight loss), in contrast to mock (PBS)-vaccinated mice, which had a body weight loss of approximately 20% by day 7 (Fig. 7A). No virus was detected in the lungs of vaccinated mice, but high virus titers were found in mock-vaccinated mice at both day 3 and day 7 postchallenge (Fig. 7B). In addition, the level of protection against HK68-MA20C challenge induced by mut+HK68-HN virus vaccination in terms of weight loss was superior to that induced by 8-mut vaccination, as expected (Fig. 5C versus 7A). Overall, this result suggests that the 8-mut virus could be used as a master donor strain to generate live attenuated vaccines.

Viral protein expression in infected cells. Since it has been proposed that codon bias may be related to translation efficiency, we evaluated whether the synonymous mutations affect protein expression in human A549 cells (Fig. 8, left). Cells were infected with WT and 8-mut viruses at an MOI of 5, and whole-cell lysates were harvested at 8 h postinfection, followed by Western blot analysis. In infected A549 cells, the level of viral protein expression of the 8-mut virus was comparable to that of the WT (±50% that of the WT). In contrast, the levels of PB2, PA, HA, NP, M1, and NS1 protein expression by the 8-mut virus were found to be much higher than the levels of expression of those proteins by the WT virus in infected DF1 cells (Fig. 8, middle and right panels). The PB1 and NA proteins could not be reliably detected by their corresponding antibodies due to the presence of nonspecific signals in DF1 cells.

Recombinant virus carrying all 8 mutated segments has the most attenuated phenotype in mammalian cells. To find out which segment was critical for virus attenuation, viruses with different combinations of wild-type and mutated segments were rescued (Table 2) and their replication kinetics in MDCK cells were studied. There was no significant difference between the growth of WT virus and viruses with any 1 mutated segment (Fig. 9A). The growth of virus with mutated vRNP (PB2, PB1, PA, and NP) segments was very similar to that of the WT (Fig. 9B), suggesting that this combination of gene segments alone was not sufficient to attenuate the virus. Interestingly, viruses carrying mutated surface protein gene segments or other internal protein gene segments were found to have moderate growth attenuation. The recombinant virus with mutated M and NS segments was found to have the most attenuation among these mutants, but its replication rate was still significantly higher than that of the original 8-mut virus

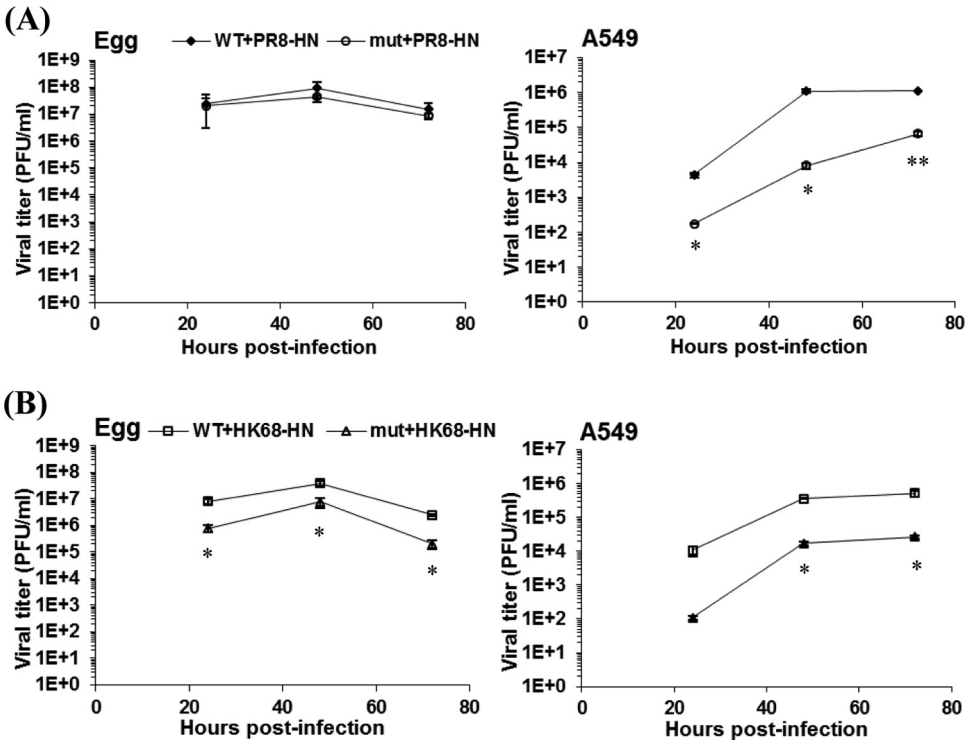

FIG 6 Growth properties of the mutant virus as a master donor strain in mammalian and avian systems. Viruses were characterized in embryonated eggs (100 PFU) and A549 cells (MOI = 0.01). The HAs and NAs of A/PR/8/34 (H1N1) (A) and A/HK/1/68 (H3N2) (B) were incorporated into the WT and mutant virus backgrounds. *, $P < 0.05$; **, $P < 0.001$.

($P < 0.05$). In addition, the plaque sizes of these mutants were still found to be larger than the plaque size of the 8-mut virus (Fig. 9C). Altogether, these results suggest that the attenuation of the 8-mut virus is contributed by multiple viral gene segments.

DISCUSSION

We have designed and synthesized a live attenuated influenza virus with an avian influenza virus codon usage bias. As hundreds of synonymous mutations were introduced into the genome (Table 1), the safety concern of reversion to a wild-type phenotype would be minimal (12). The 8-mut virus was attenuated in mammalian cells and mice but retained a replication ability in embryonated eggs comparable to that of the wild type (Fig. 2). Our method might allow codon bias vaccine candidates to be compatible with egg-based production systems. A single vaccination dose of the 8-mut virus induced various types of immune responses similar to those induced by a WT virus infection (Fig. 3). The 8-mut virus could stimulate not only a humoral response, as shown by neutralizing serum antibodies, but also a cellular response, as demonstrated by immune cell profiling, and an early innate response, as shown by beta interferon expression. Compared to the response elicited by inactivated vaccines, which can elicit only humoral immune responses, immunization with the 8-mut virus elicited a response that mimics the events in a natural infection and potentially exposes more immune targets during the replication cycle in host cells, thereby stimulating a robust protective immune response. Indeed, the 8-mut virus could induce cross-subtype protection against both homologous and heterologous viral challenges (Fig. 4 and 5).

The current commercial live attenuated vaccine consists of the master donor strain A/Ann Arbor/6/1960 with a cold-adapted phenotype (12, 39) combined with the HAs and NAs from circulating strains to update the vaccine. However, the vaccine does not stimulate a satisfactory cellular response in adults (10) and has been found to be much less efficacious than the inactivated vaccine in adults (11). The poor immunogenicity in adults was suggested to be due to previous exposure to a virus of a similar strain by annual vaccination (10, 11), which prevents replication of the vaccine virus and allows an infecting virus to evade the protective effects of the most recent vaccine. With existing sequence databases, our attenuated codon mutant virus can be designed and synthesized quickly to reflect current circulating strains and present proteins which are identical to those of the target virus. This could also avoid the stimulation of immunity targeted to the master donor strain in annual seasonal influenza vaccination, as all proteins rather than just the HA and NA reflect those of the circulating strain. More importantly, unlike the cold-adapted mutations described above, our approach would not affect the protein sequences encoded by the genomes of these viruses. Although our 8-mut virus was attenuated in human cells, it is not a temperature-sensitive mutant. Thus, this live attenuated virus can theoretically replicate in both the upper and lower respiratory tracts in humans, resulting in a more robust vaccine-induced immune response.

In the unfortunate event of an influenza pandemic, the generation of an attenuated pandemic strain for production of a vaccine by this strategy might result in additional safety concerns. In particular, in the absence of extensive virus characterization, it is pos-

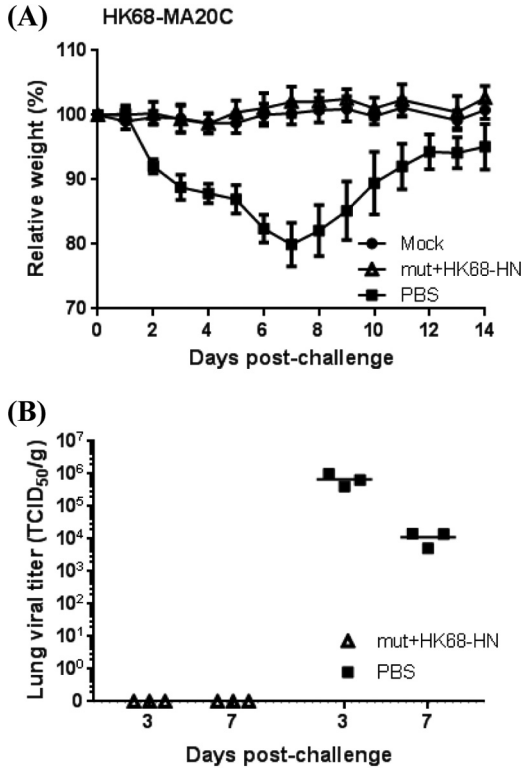

FIG 7 Protective effects caused by the mutant virus as a master donor strain. BALB/c mice were vaccinated intranasally with PBS (mock-vaccinated control) or 1×10^5 PFU of mut+HK68-HN virus. At day 28 postvaccination, mice were challenged with HK68-MA20C (6.71×10^5 PFU) or underwent mock challenge as a control. (A) The loss of body weight of 6 mice was monitored for 14 days, and data represent means ± SDs. (B) Lungs were harvested from 3 mice at 3 and 7 days postchallenge, and viral titers were determined by a $TCID_{50}$ assay on MDCK cells. Symbols represent data from individual mice.

sible that the newly emerged pandemic strain might carry unknown virulence markers in its internal genes. Therefore, it is safer to introduce the pandemic viral glycoprotein gene segments into a well-characterized attenuated vaccine master donor strain for vaccine production. Our *in vitro* and *in vivo* results have demonstrated that the BR59 mutant virus could work as a vaccine master donor strain by substitution of the HAs and NAs of other influenza viruses (Fig. 6 and 7).

The attenuation of the 8-mut virus in mammalian systems was contributed by mutations in multiple segments, as no recombinant virus with a single mutated segment had the same level of attenuation as the other recombinant viruses (Fig. 9A). Unlike other studies employing codon deoptimization or codon pair deoptimization (24–26), no significant overall reduction of proteins was found in our study (Fig. 8). The differences might be partly due to the different codon deoptimization strategies and virus strains employed and the roughly 10 times smaller amount of nucleotide mutations used in our design. One should note that altering translation efficiency is not the only host selection pressure on the viral codon usage pattern. It has been proposed that mutational pressure dominates over translation pressure in shaping codon usage in human RNA viruses, including influenza viruses (17, 18). The human seasonal influenza viruses isolated in recent years tended to have reduced GC contents in their genomes (16), perhaps to escape host antiviral responses. Moreover, synonymous mutations may have an influence on RNA base pairing, stability, and interactions with other RNAs or proteins (30). A clearer picture of the forces shaping viral codon usage has yet to be determined. The exact mechanisms responsible for the attenuation of the codon mutant viruses and their relationship to host adaptation require further investigation. Regardless of the underlying mechanisms, our attenuation strategy for vaccine virus generation was proven to be successful.

It is also interesting to note that the 8-mut virus was capable of expressing high levels of viral proteins in infected avian cells. This suggests that the newly introduced mutations can enhance viral protein expression in avian systems. We also noted, however, that the titer of this mutant virus was comparable only to that of the wild type. It is possible that in the presence of abundant viral proteins in infected cells, the availability of influenza virus proteins is no longer a rate-limiting factor for progeny virus production.

In summary, we generated a human influenza virus that has an

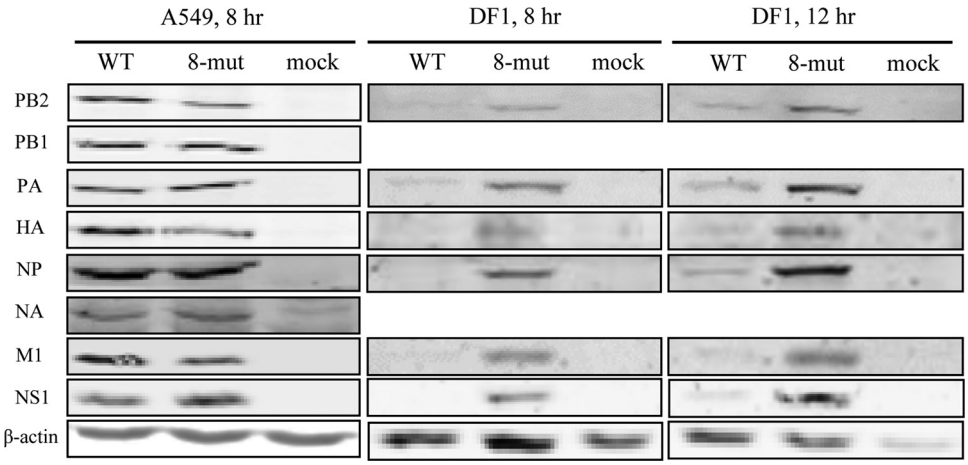

FIG 8 Expression of viral proteins in infected human A549 and DF1 cells. Cells were mock infected (mock) or infected with WT or 8-mut virus at an MOI of 5 and harvested at the indicated time points. Total cell lysates were analyzed by Western blotting using viral protein-specific antibodies, as indicated. The PB1 and NA proteins expressed in infected DF1 cells could not be reliably detected due to a high nonspecific background.

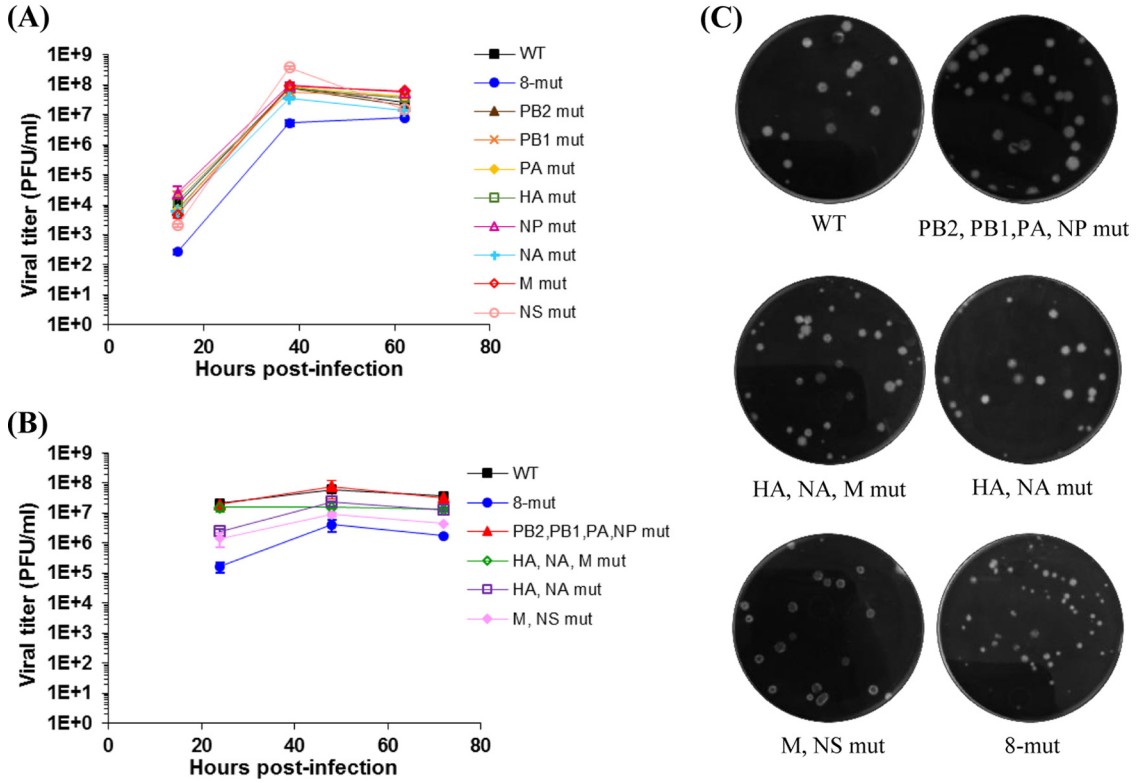

FIG 9 Growth properties of codon mutants in MDCK cells. The growth kinetics of WT and mutated viruses were characterized in MDCK cells infected at an MOI of 0.001. The replication kinetics of virus mutants containing 1 (A) or multiple (B) mutated segments (mut), as indicated, are shown. (C) Plaque sizes of recombinant viruses with multiple mutated segments, as indicated, in MDCK cells. Cells were infected, fixed, and stained with crystal violet at 3 days postinfection.

avian influenza virus codon usage bias. The mutant was attenuated in mammalian systems *in vitro* and *in vivo*, but it could replicate to high titers in embryonated eggs. This virus could stimulate a potent immune response and confer protection against homologous and heterosubtypic viral challenges. The virus could also potentially serve as a vaccine master donor strain, thereby allowing the rapid generation of vaccine strains.

ACKNOWLEDGMENTS

This project was supported by the Health and Medical Research Fund (project number 12110982) and Area of Excellence scheme AoE/M-1206.

R. L. Y. Fan and L. L. M. Poon have filed a patent application on the basis of the invention described in this study.

REFERENCES

1. **World Health Organization.** 2012. Vaccines against influenza WHO position paper—November 2012. Wkly Epidemiol Rec **87:**461–476.
2. **Michiels B, Govaerts F, Remmen R, Vermeire E, Coenen S.** 2011. A systematic review of the evidence on the effectiveness and risks of inactivated influenza vaccines in different target groups. Vaccine **29:**9159–9170. http://dx.doi.org/10.1016/j.vaccine.2011.08.008.
3. **Flannery B, Clippard J, Zimmerman RK, Nowalk MP, Jackson ML, Jackson LA, Monto AS, Petrie JG, McLean HQ, Belongia EA.** 2015. Early estimates of seasonal influenza vaccine effectiveness—United States, January 2015. MMWR Morb Mortal Wkly Rep **64:**10–15.
4. **Osterholm MT, Kelley NS, Sommer A, Belongia EA.** 2012. Efficacy and effectiveness of influenza vaccines: a systematic review and meta-analysis. Lancet Infect Dis **12:**36–44. http://dx.doi.org/10.1016/S1473-3099(11)70295-X.
5. **Belshe RB, Edwards KM, Vesikari T, Black SV, Walker RE, Hultquist M, Kemble G, Connor EM, CAIV-T Comparative Efficacy Study Group.** 2007. Live attenuated versus inactivated influenza vaccine in infants and young children. N Engl J Med **356:**685–696. http://dx.doi.org/10.1056/NEJMoa065368.
6. **Treanor JJ, El Sahly H, King J, Graham I, Izikson R, Kohberger R, Patriarca P, Cox M.** 2011. Protective efficacy of a trivalent recombinant hemagglutinin protein vaccine (FluBlok(R)) against influenza in healthy adults: a randomized, placebo-controlled trial. Vaccine **29:**7733–7739. http://dx.doi.org/10.1016/j.vaccine.2011.07.128.
7. **Yang LP.** 2013. Recombinant trivalent influenza vaccine (FluBlok(R)): a review of its use in the prevention of seasonal influenza in adults. Drugs **73:**1357–1366. http://dx.doi.org/10.1007/s40265-013-0103-6.
8. **King JC, Jr, Cox MM, Reisinger K, Hedrick J, Graham I, Patriarca P.** 2009. Evaluation of the safety, reactogenicity and immunogenicity of FluBlok® trivalent recombinant baculovirus-expressed hemagglutinin influenza vaccine administered intramuscularly to healthy children aged 6-59 months. Vaccine **27:**6589–6594. http://dx.doi.org/10.1016/j.vaccine.2009.08.032.
9. **Beyer WEP, Palache AM, de Jong JC, Osterhaus ADME.** 2002. Cold-adapted live influenza vaccine versus inactivated vaccine: systemic vaccine reactions, local and systemic antibody response, and vaccine efficacy. A meta-analysis. Vaccine **20:**1340–1353.
10. **He X-S, Holmes TH, Zhang C, Mahmood K, Kemble GW, Lewis DB, Dekker CL, Greenberg HB, Arvin AM.** 2006. Cellular immune responses in children and adults receiving inactivated or live attenuated influenza vaccines. J Virol **80:**11756–11766. http://dx.doi.org/10.1128/JVI.01460-06.
11. **Monto AS, Ohmit SE, Petrie JG, Johnson E, Truscon R, Teich E, Rotthoff J, Boulton M, Victor JC.** 2009. Comparative efficacy of inactivated and live attenuated influenza vaccines. N Engl J Med **361:**1260–1267. http://dx.doi.org/10.1056/NEJMoa0808652.
12. **Jin H, Lu B, Zhou H, Ma C, Zhao J, Yang C-F, Kemble G, Greenberg H.** 2003. Multiple amino acid residues confer temperature sensitivity to

human influenza virus vaccine strains (Flumist) derived from cold-adapted A/Ann Arbor/6/60. Virology **306:**18–24. http://dx.doi.org/10.1016/S0042-6822(02)00035-1.
13. **Plotkin JB, Kudla G.** 2010. Synonymous but not the same: the causes and consequences of codon bias. Nat Rev Genet **12:**32–42. http://dx.doi.org/10.1038/nrg2899.
14. **Li ZP, Ying DQ, Li P, Li F, Bo XC, Wang SQ.** 2010. Analysis of synonymous codon usage bias in 09H1N1. Virol Sin **25:**329–340. http://dx.doi.org/10.1007/s12250-010-3123-3.
15. **Zhou T, Gu W, Ma J, Sun X, Lu Z.** 2005. Analysis of synonymous codon usage in H5N1 virus and other influenza A viruses. Biosystems **81:**77–86. http://dx.doi.org/10.1016/j.biosystems.2005.03.002.
16. **Wong EH, Smith DK, Rabadan R, Peiris M, Poon LL.** 2010. Codon usage bias and the evolution of influenza A viruses. Codon usage biases of influenza virus. BMC Evol Biol **10:**253. http://dx.doi.org/10.1186/1471-2148-10-253.
17. **Goni N, Iriarte A, Comas V, Sonora M, Moreno P, Moratorio G, Musto H, Cristina J.** 2012. Pandemic influenza A virus codon usage revisited: biases, adaptation and implications for vaccine strain development. Virol J **9:**263. http://dx.doi.org/10.1186/1743-422X-9-263.
18. **Jenkins GM, Holmes EC.** 2003. The extent of codon usage bias in human RNA viruses and its evolutionary origin. Virus Res **92:**1–7. http://dx.doi.org/10.1016/S0168-1702(02)00309-X.
19. **Hershberg R, Petrov DA.** 2008. Selection on codon bias. Annu Rev Genet **42:**287–299. http://dx.doi.org/10.1146/annurev.genet.42.110807.091442.
20. **Aragones L, Guix S, Ribes E, Bosch A, Pinto RM.** 2010. Fine-tuning translation kinetics selection as the driving force of codon usage bias in the hepatitis A virus capsid. PLoS Pathog **6:**e1000797. http://dx.doi.org/10.1371/journal.ppat.1000797.
21. **Aragones L, Bosch A, Pinto RM.** 2008. Hepatitis A virus mutant spectra under the selective pressure of monoclonal antibodies: codon usage constraints limit capsid variability. J Virol **82:**1688–1700. http://dx.doi.org/10.1128/JVI.01842-07.
22. **Mueller S, Papamichail D, Coleman JR, Skiena S, Wimmer E.** 2006. Reduction of the rate of poliovirus protein synthesis through large-scale codon deoptimization causes attenuation of viral virulence by lowering specific infectivity. J Virol **80:**9687–9696. http://dx.doi.org/10.1128/JVI.00738-06.
23. **Coleman JR, Papamichail D, Skiena S, Futcher B, Wimmer E, Mueller S.** 2008. Virus attenuation by genome-scale changes in codon pair bias. Science **320:**1784–1787. http://dx.doi.org/10.1126/science.1155761.
24. **Yang C, Skiena S, Futcher B, Mueller S, Wimmer E.** 2013. Deliberate reduction of hemagglutinin and neuraminidase expression of influenza virus leads to an ultraprotective live vaccine in mice. Proc Natl Acad Sci U S A **110:**9481–9486. http://dx.doi.org/10.1073/pnas.1307473110.
25. **Nogales A, Baker SF, Ortiz-Riano E, Dewhurst S, Topham DJ, Martinez-Sobrido L.** 2014. Influenza A virus attenuation by codon deoptimization of the NS gene for vaccine development. J Virol **88:**10525–10549. http://dx.doi.org/10.1128/JVI.01565-14.
26. **Mueller S, Coleman JR, Papamichail D, Ward CB, Nimnual A, Futcher B, Skiena S, Wimmer E.** 2010. Live attenuated influenza virus vaccines by computer-aided rational design. Nat Biotechnol **28:**723–726. http://dx.doi.org/10.1038/nbt.1636.
27. **Moss WN, Priore SF, Turner DH.** 2011. Identification of potential conserved RNA secondary structure throughout influenza A coding regions. RNA **17:**991–1011. http://dx.doi.org/10.1261/rna.2619511.
28. **Gog JR, Afonso Edos S, Dalton RM, Leclercq I, Tiley L, Elton D, von Kirchbach JC, Naffakh N, Escriou N, Digard P.** 2007. Codon conservation in the influenza A virus genome defines RNA packaging signals. Nucleic Acids Res **35:**1897–1907. http://dx.doi.org/10.1093/nar/gkm087.
29. **Lamb RA, Takeda M.** 2001. Death by influenza virus protein. Nat Med **7:**1286–1288. http://dx.doi.org/10.1038/nm1201-1286.
30. **Priore SF, Moss WN, Turner DH.** 2012. Influenza A virus coding regions exhibit host-specific global ordered RNA structure. PLoS One **7:**e35989. http://dx.doi.org/10.1371/journal.pone.0035989.
31. **Hoffmann E, Neumann G, Kawaoka Y, Hobom G, Webster RG.** 2000. A DNA transfection system for generation of influenza A virus from eight plasmids. Proc Natl Acad Sci U S A **97:**6108–6113. http://dx.doi.org/10.1073/pnas.100133697.
32. **Xu L, Bao L, Li F, Lv Q, Ma Y, Zhou J, Xu Y, Deng W, Zhan L, Zhu H.** 2011. Adaption of seasonal H1N1 influenza virus in mice. PLoS One **6:**e28901. http://dx.doi.org/10.1371/journal.pone.0028901.
33. **Brown E, Liu H, Kit LC, Baird S, Nesrallah M.** 2001. Pattern of mutation in the genome of influenza A virus on adaptation to increased virulence in the mouse lung: identification of functional themes. Proc Natl Acad Sci U S A **98:**6883–6888. http://dx.doi.org/10.1073/pnas.111165798.
34. **Poon LL, Leung YH, Nicholls JM, Perera PY, Lichy JH, Yamamoto M, Waldmann TA, Peiris JS, Perera LP.** 2009. Vaccinia virus-based multivalent H5N1 avian influenza vaccines adjuvanted with IL-15 confer sterile cross-clade protection in mice. J Immunol **182:**3063–3071. http://dx.doi.org/10.4049/jimmunol.0803467.
35. **Valkenburg SA, Li OTW, Mak PWY, Mok CKP, Nicholls JM, Guan Y, Waldmann TA, Peiris JSM, Perera LP, Poon LLM.** 2014. IL-15 adjuvanted multivalent vaccinia-based universal influenza vaccine requires $CD4^+$ T cells for heterosubtypic protection. Proc Natl Acad Sci U S A **111:**5676–5681. http://dx.doi.org/10.1073/pnas.1403684111.
36. **Wen X, Huang X, Mok BW-Y, Chen Y, Zheng M, Lau S-Y, Wang P, Song W, Jin D-Y, Yuen K-Y, Chen H.** 2014. NF90 exerts antiviral activity through regulation of PKR phosphorylation and stress granules in infected cells. J Immunol **192:**3753–3764. http://dx.doi.org/10.4049/jimmunol.1302813.
37. **Blaschke V, Reich K, Blaschke S, Zipprich S, Neumann C.** 2000. Rapid quantitation of proinflammatory and chemoattractant cytokine expression in small tissue samples and monocyte-derived dendritic cells: validation of a new real-time RT-PCR technology. J Immunol Methods **246:**79–90. http://dx.doi.org/10.1016/S0022-1759(00)00304-5.
38. **Nicholls JM, Wong LPW, Chan RWY, Poon LLM, So LKY, Yen H-L, Fung K, van Poucke S, Peiris JSM.** 2012. Detection of highly pathogenic influenza and pandemic influenza virus in formalin fixed tissues by immunohistochemical methods. J Virol Methods **179:**409–413. http://dx.doi.org/10.1016/j.jviromet.2011.11.006.
39. **Maassab H.** 1969. Biologic and immunologic characteristics of cold-adapted influenza virus. J Immunol **102:**728–732.